Optimization of Multiple Receivers Solar Power Tower systems

E. Carrizosa[a,b], C. Domínguez-Bravo[b,*], E. Fernández-Cara[b,c], M. Quero[d]

[a] *Department of Statistics and Operations Research, University of Seville, Spain*
[b] *Mathematics Institute of the University of Seville, Spain*
[c] *Department of Partial Equations and Numerical Analysis, University of Seville, Spain*
[d] *Abengoa Solar New Technologies, Seville, Spain*

Abstract

In this article a new procedure to optimize the design of a solar power tower system with multiple receivers is presented. The variables related to the receivers (height, aperture tilt angle, azimuth angle and aperture size) as well as the heliostat field layout are optimized seeking to minimize the levelized cost of thermal energy. This is a high dimensional optimization problem with black-box nonconvex objective function.

The proposed strategy alternatively optimizes the receivers and the heliostat field. A separate aiming region is considered for each receiver. The aiming regions, the number of heliostats and their locations are obtained with the proposed procedure. Specifically, heliostat positions are obtained through a pattern-free greedy-based location method.

Keywords: solar thermal power, heliostat field layout, nonconvex

*Corresponding author.
Instituto de Matemáticas de la Universidad de Sevilla (IMUS)
Edificio Celestino Mutis- 1 Planta- D10.5
Avda. Reina Mercedes, s/n, 41012 Sevilla, Spain.
Tel: +34 955420870.
Email address: carmenanadb@us.es (C. Domínguez-Bravo)

optimization, greedy algorithm, multiple receivers

1. Introduction

SPT (Solar Power Tower) systems are known as one of the most promising technologies for producing solar electricity, as claimed in the literature [1, 2, 3]. An SPT system is here considered to consist of three main components: a tower, one or several receivers and a field of heliostats comprising rectangular mirrors. Direct solar radiation is reflected and concentrated by the heliostat field onto the receivers, placed at the top of the tower. The heliostats have two-axis movement in order to reflect the direct light from the sun to fixed targets on the receivers. The thermal energy is transferred in the receivers to a heat conducting fluid and, then, electricity is produced through a conventional thermodynamic cycle.

In recent years, higher power requirements are imposed on the SPT systems calling for large-scale plants such as Gemasolar (19.9 MW and 2650 hel. [4, 5]), Khi Solar One (50 MW and 4120 hel. [6]) and Ivanpah (377 MW and 173500 hel. [7, 8]). Using one-receiver systems, as pointed out in [9, 10, 11], the large amount of heliostats forces to locate heliostats far from the tower, increasing atmospheric and spillage losses. The use of multiple receivers systems allows to reach high temperatures required to achieve conversion efficiency of solar energy to electricity, see [12].

Regarding the spatial configurations of the multiple receivers, there are different proposals in the literature: vertical [13], circular [14, 15], same focal spot [16] and horizontal, see [10, 17].

In what concerns the heliostat field layout, different approaches have also

been studied in the literature, see [18, 9, 12, 13, 10, 17]. A common approach relies on the field separation method: for each receiver a separate region, called aiming region is identified, where the heliostats will we placed, see [18].

This method is mainly based on two facts: the varying heliostats performance regarding their position in the field [11], and the computational time reduction by implementing simplified methods to calculate shading and blocking effects [19, 20]. If, for instance, we consider three aiming regions, namely North, West and East, the West region will be most efficient at the beginning of the day and the East region in the afternoon. These performances imply that the optimal number and density of heliostats will not necessarily be the same for each selected region.

Different shapes are usually imposed to the aiming regions, such as concentric circular trapezoids [13] or ellipses [10, 17]. However, such aiming regions overlap, and it is not trivial how to fix a strategy to assign heliostats at the intersection of the regions.

The heliostat location problem is usually solved by applying a parameterized geometrical pattern. The pattern parameters are optimized and the final number of heliostats is obtained by oversizing the field, see [10]. This way, although the optimal parameters for the oversized field are obtained, there is a high risk that a strong distortion exists between the original and final configuration. The field separation strategy has already been used under radially-staggered layouts in [11].

Finally, in order to design the SPT system, it is essential to understand the performance of the subsystems formed by the receivers and the heliostat field. The field and the receivers are interdependent, as pointed out in [13],

where it is shown that an increase of the height of a receiver reduces some optical losses (shading, blocking and cosine effects) in large heliostat fields. It is thus important to design both components simultaneously.

This coupled optimization problem has been addressed in the literature by different authors. In [10], a genetic-based algorithm is proposed to optimize the radial-stagger field layout parameters, the tower height and the receiver aperture size and tilt angle. In [9], 11 design variables are optimized through a variant of the Powell algorithm and a genetic-based algorithm. In a different way, in [11] the receiver is firstly selected to be as simple and cheap as possible, and then the radial-staggered field is limited to a ellipsoidal boundary which size is determined by the receiver. Finally, in [13], a reference field is fixed and the two receivers considered are placed in the best vertical arrangement found. Then, different 2-zones heliostat field configurations are evaluated and the one reaching the best plant performance is selected.

In this article a new method to design a multiple receivers SPT system is presented, where the receivers and the heliostat field layout are simultaneously optimized. The variables related to the receivers and the heliostats (number and positions) are optimized through an alternating process to obtain a multiple receivers system that minimizes the *levelized cost of thermal energy* (LCOE).

The spatial configuration selected for the multiple receivers system is the horizontal distribution, and each receiver is characterized by its own height in the tower, aperture tilt angle, azimuth angle and aperture radius, see Figure 1.

The separation method is applied to design the field layout and each aiming region is obtained by the algorithm without imposing any particular shape. For simplicity, the heliostats are considered aiming the same receiver regardless the instant of time.

The methodology presented to solve the heliostat location problem is a greedy-based algorithm which does not impose geometric patterns for the heliostats locations and does not fix in advance the number of heliostats. In a greedy algorithm, solutions are progressively built by incorporating at each iteration a new element (heliostat) until a complete feasible solution is obtained. The selection of the new element follows a greediness criterion seeking improvement of the objective function at each individual step. Although optimization based on a pure greedy heuristic may not necessarily be optimal, e.g. [21], it is frequently used in combinatorial optimization theory and practice. Its common use may be due to its simplicity, and, as stated in such paper, due to the fact that it is widely assumed that it often provides solutions that are significantly better than the worst ones. See e.g. [22, 23, 24, 25], for results of the greedy algorithm on a bunch of combinatorial optimization problems.

The spatial configuration selected for the multiple receivers system is the horizontal distribution, and each receiver is characterized by its own height in the tower, aperture tilt angle, azimuth angle and aperture radius, see Figure 1. As far as the authors are aware of, these are novel issues in the literature.

The rest of the paper is organized as follows. In Section 2, the SPT system is presented. Section 3 explains the optimization problem and our

methodology to solve it. We apply the proposed algorithms to a given configuration and discuss the main results in Section 4. The last section is devoted to summarize our results and to present some perspectives for further work.

2. Decision Variables and Functions

The optimal design of a multiple receivers SPT system consists of determining the apertures dimensions and receivers positions in the tower and the location of the heliostats so as to minimize the LCOE. In the following subsections, the variables, the feasible sets and the functions involved in the optimization problem will be presented.

2.1. Decision variables

In the chosen system of coordinates, the positive x axis is the North direction, the positive y axis is the West direction and the z axis is orthogonal to the ground. We deal with cavity receivers with circular aperture, see Figure 1(a) and [1] for further details. Although our approach is valid for any number of receivers, we consider for simplicity three receivers, called North, West and East, and numbered as receiver 1, 2 and 3 respectively.

The four most relevant variables associated to each receiver design are considered, namely the *height* h in the tower, the aperture *tilt* angle ξ (which measures the separation from the vertical line), the *azimuth* angle α (which measures the separation from the North axis) and the aperture *radius* r, see Figures 1(a)-1(b). From now on we will denote by Θ_i the optimization variables related to receiver i and by Θ the full collection of decision variables concerning the receivers:

$$\Theta = (\Theta_1, \Theta_2, \Theta_3) \in \mathcal{M}_{4\times 3} \text{ with } \Theta_i = (h_i, \xi_i, \alpha_i, r_i)^t \in \mathbb{R}^4 \quad \forall\, i = 1, 2, 3\,. \quad (1)$$

Some constraints, influenced by technical and legal regulations, determine the feasible region $\mathbf{\Theta}$. They are written as follows:

$$\mathbf{\Theta} := \left\{ \begin{array}{ll} \Theta \in \mathcal{M}_{4\times 3} : & r_{min} \leq r_i \leq \min(h_i, r_{max}) \leq h_{max} \quad \forall\, i = 1,2,3 \\ & \xi_i \in [0, \pi/2] \\ & \alpha_i \in [\underline{\alpha}_i, \overline{\alpha}_i] \end{array} \right\} . \quad (2)$$

Here, r_{min} and r_{max} denote the minimum and maximum receiver radius and h_{max} is the maximum value for the tower height. The ranges for the variables α_i are calculated as follows:

$$\begin{array}{ll} \underline{\alpha}_1 = \max\{-\pi/2, \alpha_3 + \varsigma_3 + \varsigma_1\}\,, & \overline{\alpha}_1 = \min\{\pi/2, \alpha_2 - \varsigma_2 - \varsigma_1\}\,, \\ \underline{\alpha}_2 = \max\{0, \alpha_1 + \varsigma_1 + \varsigma_2\}\,, & \overline{\alpha}_2 = \min\{\pi, \alpha_3 - \varsigma_3 - \varsigma_2\}\,, \\ \underline{\alpha}_3 = \max\{-\pi, 2\pi + \alpha_2 + \varsigma_2 + \varsigma_3\}\,, & \overline{\alpha}_3 = \min\{0, \alpha_1 - \varsigma_1 - \varsigma_3\}\,, \end{array} \quad (3)$$

where the angles ς_i are obtained through the following equations:

$$\varsigma_i = \arcsin\left(\frac{r_i}{\sqrt{r_i^2 + d_{\text{ap}}^2}}\right) \quad \forall\, i = 1,2,3\,. \quad (4)$$

The fixed parameter d_{ap} denotes the distance between each aperture and the center of coordinates, see Figures 1(a)-1(c).

In what concerns the field, the heliostat locations, given by the coordinates (x, y) of their centers, are the variables to be used. All heliostats are assumed to be rectangular, to have the same dimensions and to be composed of rectangular facets; see [26, 27] for approaches where heliostats of different sizes are allowed. The finite collection of coordinates of the centers of the heliostats defines the heliostat field $\mathcal{S}$. The heliostats must be located within

a given region $\Omega \subset \mathbb{R}^2$ and they have to rotate freely avoiding collisions between them. The feasible region $\mathscr{S}$ is:

$$\mathscr{S} := \left\{ \begin{array}{ll} \mathcal{S} \subset \Omega : & |\mathcal{S}| < +\infty \\ & ||(x,y)-(x',y')|| \geq \delta \quad \forall\, (x,y),(x',y') \in \mathcal{S} \\ & \qquad\qquad\qquad\qquad (x,y) \neq (x',y') \end{array} \right\}, \tag{5}$$

where $\delta > 0$ is a given positive parameter, called security distance. Note that the variable $\mathcal{S}$ is a set whose cardinality is not fixed in advance.

As already mentioned, we assume that each heliostat is always aiming at the same receiver. The separate heliostat fields, denoted by $\mathcal{S}_i$ for $i = 1, 2, 3$, are expressed as follows:

$$\mathcal{S}_i := \{(x,y) \in \mathcal{S} \,:\, \text{heliostat at } (x,y) \text{ aims at receiver } i\} \;\text{ with } \mathcal{S} = \bigcup_{i=1}^{3} \mathcal{S}_i \,. \tag{6}$$

2.2. Functions

The function to be optimized, called the levelized cost of thermal energy (LCOE), is an aggregation of two criteria, namely, the total investment cost and the thermal energy collected by the field.

The investment cost C takes into account the investment in the solar power plant equipment (tower, receivers and heliostats). Hence, it depends on the receiver variable Θ, and the number of heliostats in the field $|\mathcal{S}|$, as follows:

$$C(\Theta, |\mathcal{S}|) := \beta_1 (\max_i \{h_i\} + \kappa)^\sigma + \beta_2 \pi \sum_{i=1}^{3} r_i^2 + c_F + c|\mathcal{S}| \,, \tag{7}$$

where β_1 and β_2 are empirical constants with values in $(0,1)$, κ and σ are positive and given by appropriate physical considerations and c denotes the cost per heliostat. For simplicity, the cost associated to the land (purchasing and preparing) is considered fixed and denoted by c_F.

The thermal annual energy collected by the field into the receiver is calculated following [28], which is based in the NSPOC procedure [19] with 12 representative days considered. In this paper, however, a slight change is done: instead of using a polynomial fitting to obtain the annual value, the rectangular quadrature rule is applied since we proceed in practice at each receiver individually. The thermal annual energy E function takes the form:

$$E(\Theta, \mathcal{S}) := \int_0^T \Pi_t(\Theta, \mathcal{S})\, dt - \gamma_1\,, \tag{8}$$

where t denotes the time instant, Π_t is the outlet thermal power collected at time t, calculated as in [28, 29, 19], and γ_1 is a constant that measures the fixed energy losses related to the whole system.

Finally, the LCOE of the system is given by

$$F(\Theta, \mathcal{S}) := C(\Theta, |\mathcal{S}|)/E(\Theta, \mathcal{S})\,. \tag{9}$$

It is clear that F is a quantity that, at least at first sight, furnishes global information on the overall advantages and disadvantages of the inversion needed to produce energy. Consequently, it is completely natural to try to minimize F.

The approach proposed in this paper uses such calculations as subroutines and could thus be replaced by any alternative method such as e.g. ray-tracing methods [30].

3. Problem Statement

Our goal is to design an SPT system with multiple receivers technology in order to minimize the LCOE of the system. Usually, when designing an SPT system, a fixed time instant is used to size the plant, as explained in [28, 13]. This time instant, denoted by T_d, is known in the literature as the *design point*. At $t = T_d$, a minimal and a maximal power for each receiver are required, that is:

$$\Pi_i^- \leq \Pi_{T_d}(\Theta_i, \mathcal{S}) \leq \Pi_i^+ \quad i = 1, 2, 3\,. \tag{10}$$

Including these constraints, the optimization problem is written as follows:

$$(\mathcal{P}) \begin{cases} \min\limits_{\Theta, \mathcal{S}} & F(\Theta, \mathcal{S}) = C(\Theta, |\mathcal{S}|)/E(\Theta, \mathcal{S}) \\ \text{subject to} & \Theta \in \mathbf{\Theta} \\ & \mathcal{S} \in \mathscr{S} \\ & \Pi_i^- \leq \Pi_{T_d}(\Theta_i, \mathcal{S}) \leq \Pi_i^+ \quad i = 1, 2, 3\,. \end{cases} \tag{11}$$

The characteristics of the objective function are challenging: nonconvex, black-box type, computationally expensive and high number of variables (thousands of heliostats in commercial plants, see [5]), making this problem difficult to solve.

Two blocks of decision variables are considered: those related to the design of the receivers Θ, and those related to the field layout $\mathcal{S}$.

In order to handle problem $(\mathcal{P})$, we first split it in two subproblems: the *Multiple Receivers Optimization* and the *Field Optimization*. The multiple receivers optimization problem, denoted by $(\mathcal{P}_\mathcal{S})$, describes the optimization

of the multiple receivers when the heliostat field is fixed. Contrarily, the field optimization problem, denoted by $(\mathcal{P}_\Theta)$, describes the field optimization for a fixed multiple receivers configuration.

Both subproblems are solved independently (following specific methods described in next subsections) and, finally, an alternating method is applied to obtain a solution of the complete problem $(\mathcal{P})$.

The alternating algorithm, described in Figure 2 and Algorithm 1, starts with an initial feasible solution $(\Theta^0, \mathcal{S}^0)$ and sequentially optimizes subproblems $(\mathcal{P}_\mathcal{S})$ and $(\mathcal{P}_\Theta)$. We say that the alternating algorithm performs an iteration when both subproblems are solved. The optimization process is repeated until the value of the objective function increases or the difference between two consecutive iterates is irrelevant, that is, $||F(\Theta^k, \mathcal{S}^k) - F(\Theta^{k+1}, \mathcal{S}^{k+1})|| \leq \epsilon_0$ for a given ϵ_0. See [28], for further details on the application of this approach to a one-receiver system.

Observe that the cardinality of $\mathcal{S}$ is not fixed in advance in problems $(\mathcal{P})$ and $(\mathcal{P}_\Theta)$. Thus, we cannot express them as standard optimization problems in fixed dimension. In the following subsections we present strategies devised to solve problems $(\mathcal{P}_\Theta)$ and $(\mathcal{P}_\mathcal{S})$ independently.

3.1. Multiple Receivers Optimization

We are going to focus on the first subproblem $(\mathcal{P}_\mathcal{S})$, where the heliostat field is considered fixed and the optimization variables are those connected to the multiple receivers configuration:

$$(\mathcal{P}_{\mathcal{S}}) \quad \mathcal{S} \text{ fixed} \begin{cases} \min\limits_{\Theta} & F(\Theta, \mathcal{S}) \\ \text{subject to} & \Theta \in \mathbf{\Theta} \\ & \Pi_i^- \leq \Pi_{T_d}(\Theta_i, \mathcal{S}) \leq \Pi_i^+ \quad i = 1, 2, 3\,. \end{cases} \tag{12}$$

In general, to solve subproblem $(\mathcal{P}_{\mathcal{S}})$ we apply the Multiple Receivers Algorithm described in Algorithm 2. This algorithm performs an iteration once all the receivers have been optimized. The algorithm stops after an iteration when no improvement in the objective function is found or the difference between the obtained configuration and the previous one is insignificant, i.e. $||\Theta^k - \Theta^{k+1}||_\infty \leq \epsilon_1$ for a given ϵ_1. The power requirements are included in the objective function by penalizing the non-feasible solutions.

Individually, the different receivers are optimized sequentially, and the set of variables associated to each receiver Θ_i are optimized using the cyclic coordinate method. This method performs at each receiver variable (h_i, ξ_i, α_i and r_i) a local search in the corresponding feasible interval given by the feasible set $\mathbf{\Theta}$ described in (2). While optimizing receiver i the following stopping rule is applied: $||\Theta_i^k - \Theta_i^{k+1}||_\infty \leq \epsilon_2$ for a given ϵ_2. In other words, the cyclic coordinate method stops when the difference between two consecutive solutions is irrelevant, see [31] for further details.

3.2. Field Optimization

We are going to focus now on the heliostat field optimization subproblem, when the variables related to the receiver are fixed, that is, the resolution of problem $(\mathcal{P}_\Theta)$:

$$(\mathcal{P}_\Theta) \quad \Theta \text{ fixed} \begin{cases} \min\limits_{\mathcal{S}} & F(\Theta, \mathcal{S}) \\ \text{subject to} & \mathcal{S} \in \mathscr{S} \\ & \Pi_i^- \leq \Pi_{T_d}(\Theta_i, \mathcal{S}) \leq \Pi_i^+ \quad i = 1, 2, 3\,. \end{cases} \tag{13}$$

This is a difficult large-dimensional multimodal black-box optimization problem. Therefore, heuristic methods are applicable. These do not necessarily guarantee that we find a globally optimal solution, but are fast enough and do not require much knowledge about the function itself. For simplicity, three receivers and a different aiming region for each receiver are considered. The resolution of problem $(\mathcal{P}_\Theta)$ is divided in two stages: the division of the feasible region Ω into three aiming regions and the location of heliostats within each aiming region.

Aiming regions calculation.

Given a multiple receivers configuration Θ, the field optimization procedure starts by discretizing the feasible region Ω in order to separate it into three regions of empty intersection. Firstly, for each point (x, y) of the discretization, the energy generated by a heliostat centered at (x, y) and aiming at receiver i, for $i = 1, 2, 3$, is calculated. Then, the optimal aiming of this point, if no other heliostat existed in the field, is identified as the receiver where the maximum thermal energy is collected, i.e. receiver j if $j = \arg\max\limits_i \{E(\Theta_i, \{(x, y)\})\}$.

This section is illustrated with some examples obtained after applying the proposed method to an annulus shaped feasible region Ω and the following multiple receivers configuration:

$$\Theta = \begin{pmatrix} 100.5 & 100.5 & 100.5 \\ 12.5 & 12.5 & 12.5 \\ 0 & 90 & -90 \\ 6.39 & 6.39 & 6.39 \end{pmatrix}, \tag{14}$$

with units detailed in Table 2.

Since Ω is infinite, a finite grid is chosen in the discretization, obtaining plots such as the one in Figure 3(a), yielding the maximum energy values, and Figure 3(b), yielding the split given by the optimal aiming: red, black and blue correspond to the West, North and East receiver.

Once a discretization of Ω is obtained, the three sets of boundary points are selected and a polynomial fit is applied to each set. Three polynomial fits are applied to the following boundary points: North-West, North-East and West-East; obtaining p, q and s polynomials respectively. In the given example, the south region is fairly separated by the x axis as can be seen in Figure 3(a).

The regions have not the same influence over the objective function. North region reaches better values if we are in the northern hemisphere, see Figure 3(a) and different power requirements are considered for each receiver. A simple process without considering different possible regions may not lead to the best field configuration. Therefore, different weights are applied to the obtained energy values in order to give more or less priority to the northern region. That is, for each point (x, y) and each weight $w \in \mathbb{R}^+$, the optimal aiming is calculated as the receiver where the maximum value is achieved, i.e. $\max\{wE(\Theta_1, \{(x, y)\}), E(\Theta_2, \{(x, y)\}), E(\Theta_3, \{(x, y)\})\}$.

Given the weight $w \in \mathbb{R}^+$ and following the previous notation, each aim-

ing region is denoted by Ω_i^w and expressed as follows:

$$\Omega_1^w = \left\{ \begin{array}{ll} (x,y) \in \Omega : & x \geq 0 \\ & q_w(x) \leq y \leq p_w(x) \end{array} \right\}, \tag{15}$$

$$\Omega_2^w = \left\{ \begin{array}{lll} (x,y) \in \Omega : & y \geq p_w(x) & \text{if } x \geq 0 \\ & y \geq s_w(x) & \text{if } x < 0 \end{array} \right\}, \tag{16}$$

$$\Omega_3^w = \left\{ \begin{array}{lll} (x,y) \in \Omega : & y \leq q_w(x) & \text{if } x \geq 0 \\ & y \leq s_w(x) & \text{if } x < 0 \end{array} \right\}. \tag{17}$$

As a first example, w is set to 1, i.e. no prioritized region is considered. After applying the procedure, p_1, q_1 and s_1 are obtained as shown in Figure 3(c), where the West-East polynomial s_1 corresponds to the x axis. If five different weights $w_k \in \mathbb{R}_+$ are considered, for each weight we obtain the corresponding three polynomials p_{w_k}, q_{w_k} and s_{w_k}, which define three different aiming regions. As can be seen in Figure 3(d), considering $w = 1.010$ (resp. $w = 0.990$), more priority (resp. less priority) is given to the North region.

Then, the heliostat location problem is solved for the aiming regions obtained corresponding to the various weights. At the end of the process, the field layout which reaches the best objective value is selected as final solution.

Heliostats location.

Once the three aiming regions are obtained for a given weight w, our second goal is to calculate the heliostat field layout, that is, $\mathcal{S}_i \in \mathscr{S}_i^w$, where the feasible sets are given by $\mathscr{S}_i^w = \mathcal{S} \cap \Omega_i^w$ for $i = 1, 2, 3$. The algorithm starts locating heliostats at the most favorable region (Ω_1^w if we are in the

northern hemisphere) leading to $\mathcal{S}_1$. This first location problem is denoted by $(\mathcal{P}^1_\Theta)$ and is described below:

$$(\mathcal{P}^1_\Theta) \quad \Theta \text{ fixed} \begin{cases} \min\limits_{\mathcal{S}_1} & F(\Theta, \mathcal{S}_1) \\ \text{subject to} & \mathcal{S}_1 \in \mathscr{S}_1^w \\ & \Pi_{T_d}(\Theta_1, \mathcal{S}_1) \geq \Pi_0^1 \,. \end{cases} \tag{18}$$

After $\mathcal{S}_1$ is obtained, the procedure continues by solving $(\mathcal{P}^2_\Theta)$ and $(\mathcal{P}^3_\Theta)$ simultaneously, to obtain $\mathcal{S}_2$ and $\mathcal{S}_3$. For $i = 2, 3$, both problems are described below.

$$(\mathcal{P}^i_\Theta) \quad \Theta \text{ fixed} \begin{cases} \min\limits_{\mathcal{S}_i} & F(\Theta, \mathcal{S}) \\ \text{s.t.} & \mathcal{S}_i \in \mathscr{S}_i^w \\ & ||(x,y) - (x',y')|| \geq \delta \quad \forall\, (x,y) \in \mathcal{S}_i \,,\, (x',y') \in \mathcal{S}_1 \\ & \Pi_{T_d}(\Theta_i, \mathcal{S}_i) \geq \Pi_0^i \,. \end{cases} \tag{19}$$

Note that problem $(\mathcal{P}^i_\Theta)$ includes constraints motivated by the heliostat positions from $\mathcal{S}_1$. Collisions between heliostats must be avoided including those located near the boundaries of the aiming regions.

Following the location algorithm described later on, at a first phase the heliostats are located at each aiming region until the minimal power requirement for the corresponding receiver is reached. This step is called the *Requirement Phase*, where a feasible solution of problem $(\mathcal{P}_\Theta)$ is obtained.

However, a second phase called *Completion Phase* is applied where the location of the heliostats continues if the value of the objective function improves and the maximal power requirement is not attained. Unlike the

requirement phase where heliostats are located at the corresponding aiming region, in the completion phase the three aiming regions are considered simultaneously and the heliostats are located at the best of one of the three possible positions if and only if the objective value of the system improves and the maximal power requirements are not attained. If none of the three new positions improves the LCOE of the system or any of the maximal power requirements is achieved, the algorithm stops and gives as solution the field obtained so far.

We give now a briefly explanation of the algorithm used to solve the different heliostats location problems ($\mathcal{P}^i_\Theta$) for $i = 1, 2, 3$. It is a pattern-free greedy-based location algorithm applied in [28] with one-receiver systems. This Greedy Algorithm locates the heliostats one by one at the best position of the selected region. At each step of the algorithm a new heliostat is introduced in the field modifying the shading and blocking effects and taking into account the constraints of the heliostats already located.

For several reasons, this strategy seems very reasonable: at each step, the number of variables with respect we minimize is small, which allows a quick resolution; moreover, it permits to determine the total amount of heliostats without any a priori requirement. Furthermore, it has been tested successfully in the framework of one-receiver fields, see [28].

The complete heliostat location algorithm proposed to solve problem ($\mathcal{P}_\Theta$) is detailed in Algorithm 3. Note that $\left(\mathcal{P}^i_\Theta\right)^k$ denotes the problem of locating heliostat number k at the aiming region i, where there are already $k-1$ heliostats. At each step of the algorithm, the corresponding field is updated with the new position obtained by the Greedy Algorithm. In the requirement

phase, the North field is first calculated followed by the East and West fields, that are calculated simultaneously reducing the computational time. Then, in the completion phase, the final number of heliostats and the final field are obtained.

Following the example with weight $w = 0.990$, after the *Requirement Phase* the algorithm gives as solution the field shown in Figure 4(a), where heliostats aiming different receivers are highlighted with different colors, and heliostats located at the *Completion Phase* are highlighted with white asterisks. The product of the efficiency coefficients (cosine, shading and blocking, interception and atmospheric) for each heliostat at different time instants are shown in Figure 4(b)-4(d), where the different variations over the day can be appreciated.

4. Results

The SPT system is assumed to be placed at the same location of the reference plant called **PS10**, see [32]. In Table 1, all the fixed parameters are detailed. The lack of results available in the literature in this multiple receivers approach has made impossible to carry out a comparison of the obtained results with possible competitors. All the algorithms have been implemented in Matlab to have a user-friendly and easily adaptable prototype.

We detail in this section the iterations performed by the proposed alternating algorithm. As detailed in Section 3.2-Figure 3(d), we have considered five different weights in previous experiments and the best results were found with $w = 0.990$. We maintain this value constant, and we apply the Alternating algorithm taking as initial solution Θ^0, detailed in Table 2. The

minimal and maximal power requirements are set to $\Pi^0 = 38.27\ MWth$ and $\Pi^+ = 40.18\ MWth$ respectively and equal for the three receivers.

The Alternating algorithm performs three complete iterations and stops when $||F(\Theta^1, \mathcal{S}^1) - F(\Theta^2, \mathcal{S}^2)|| < \epsilon_0$, with $\epsilon_0 = 0.001$. The three heliostat fields obtained during the process, $\mathcal{S}^0$, $\mathcal{S}^1$ and $\mathcal{S}^2$, are shown in Figures 4(a)-5(a)-5(b), respectively. Regarding the multiple receivers optimization algorithm, the stopping parameters are set as $\epsilon_1 = \epsilon_2 = 0.1$.

As shown in Table 3 and Figure 6, applying the algorithm a reduction on the LCOE value is achieved. Note that the label enumeration corresponds with the configurations detailed in Table 3 (column 2) and that heliostats aiming different receivers are highlighted with different colors.

During the optimization process (see Table 2), the aperture sizes are reduced and the receivers positions are modified, unlike the receivers height, that remains approximately constant. The aiming regions, location and number of heliostats in the different fields have also been modified by the algorithm according to the receivers changes. The final solution is configuration number 3 which corresponds with $(\Theta^1, \mathcal{S}^1)$ where the minimum LCOE value is achieved.

Note that due to the differences between the azimuth angles of East and West receivers in the different iterations, the location of heliostats in the southern part of the field changes. With the initial solution Θ^0, where receivers East and West have a bigger azimuth angle, heliostats are located in the southern part, see field $\mathcal{S}^0$. However, with configurations Θ^1 and Θ^2 (smaller azimuth angle between the receivers) the number of heliostats located in the southern region is reduced, see fields $\mathcal{S}^1$ and $\mathcal{S}^2$.

Regarding the obtained heliostat field layouts, some irregularities appear at the boundaries. The shape of the final field could be smoothed by using, for instance, a nonrestricted refinement method [33] or selecting continuous piecewise linear polynomials to better adapt the boundaries discontinuities.

The provided results are not yet validated through an experimental or equivalent procedure and they may not be verified. However, our computational experience shows how promising our new method is for this kind of problems.

5. Conclusions and further work

In this article, a method to design multiple receivers SPT systems is proposed, where the receivers and the heliostat field are simultaneously optimized. The method identifies the aiming areas (field areas with the same aiming receiver) and calculates their boundaries without imposing any fixed shape. Heliostats are located freely at different regions following a pattern-free procedure called Greedy Algorithm.

The proposed method is applied with a three receivers initial configuration showing that the design of multiple receivers systems can be optimized using pattern-free strategies. A new heliostat field layout and a new multiple receivers configuration are obtained at the end of the process successfully reducing the LCOE value of the initial configuration.

Several extensions of this work are possible, in some cases with not much effort. Throughout the paper we have considered independent power threshold levels for the different receivers, each measured at one (common) design point. It is straightforward to extend our method to the case in which overall

power threshold levels, or multiple design points are considered. The calculation of the optimal number of receivers and their related variables is another possible extension.

In our approach, we have assumed a homogeneous flux distribution, see [16]. However, differences in flux density will occur over the absorber area and the distribution will also vary during the day and the seasons. An appropriate control is required to adapt the mass flow in the absorber to the solar distribution. The design of an appropriate aiming strategy yields a continuous nonlinear constrained black-box optimization problem of very large dimensions which deserves further analysis, see for instance [34, 35].

The field has been designed so that one natural performance, the LCOE, is optimized. However, solving the optimization problem with various objective functions is also possible. See for instance [36] for a multi-objective thermoeconomic optimization approach with one single receiver.

Finally, we have considered all the receivers to be located at the same (unique) tower. Multi-towers configurations are an interesting innovation in SPT systems, see [37]. The calculation of the optimal towers positions and the aiming strategies to be applied are the major additional difficulties. This may be addressed through an adapted application of the methods presented here.

6. Acknowledgments

This research has been mainly supported by Abengoa Solar N.T. and Institute of Mathematics of University of Seville (IMUS), through the research contract "CapTorSol". The authors would also like to acknowledge the sup-

port from the Government of Spain (Grants MTM2012-36136, MTM2013-41286-P), Andalucía (Grant P11-FQM-7603) and EU COST Action TD1207.

References

[1] O. Behar, A. Khellaf, and K. Mohammedi. A review of studies on central receiver solar thermal power plants. *Renewable and Sustainable Energy Reviews*, 23:12–39, 2013.

[2] D. R. Mills. Advances in solar thermal electricity technology. *Solar Energy*, 76:19–31, 2004.

[3] M. Romero, R. Buck, and J. E. Pacheco. An update on Solar Central Receiver Systems, Projects and Technologies. *Journal of Solar Energy Engineering*, 124:(11 Pages), 2002.

[4] SolarPACES-NREL. Gemasolar thermosolar plant. Technical report, Sener, 2011. URL `www.nrel.gov/csp/solarpaces/project_detail.cfm/projectID=40`.

[5] J. I. Burgaleta, S. Arias, and D. Ramirez. GEMASOLAR, the first tower thermosolar commercial plant with molten salt storage. In *Proceedings of SolarPaces 2011*, 2011.

[6] SolarPACES-NREL. Khi solar one. Technical report, Abengoa Solar, 2014. URL `www.nrel.gov/csp/solarpaces/project_detail.cfm/projectID=244`.

[7] SolarPACES-NREL. Ivanpah solar electric generating system. Technical report, BrightSource Energy, 2014. URL www.nrel.gov/csp/solarpaces/project_detail.cfm/projectID=62.

[8] BrightSource. Ivanpah solar electric generating system. Technical report, BrightSource, 2014. URL www.brightsourceenergy.com/stuff/contentmgr/files/0/3eac1a9fed7f13fe4006aaab8c088277/attachment/ivanpah_white_paper_0414.pdf.

[9] A. Ramos and F. Ramos. Strategies in Tower Solar Power Plant optimization. *Solar Energy*, 86:2536–2548, 2012.

[10] M. Schmitz, P. Schwarzbözl, R. Buck, and R. Pitz-Paal. Assesment of the potencial improvement due to multiple apertures in central receiver systems with secondary concentrators. *Solar Energy*, 80:111–120, 2006.

[11] A. Segal and E. Teufel. Optimum layout of heliostat field when the tower-top receiver is provided with secondary concentrators. Technical report, Weizmann Institute of Science (SFERA), 2012. URL http://sfera.sollab.eu/downloads/JRA/WP13/R13.3b_SFERA_WP13T2_Opt_HelioField_Secondary_TopReceiver.pdf.

[12] A. Rovira, M. J. Montes, M. Valdes, and J. M. Martínez-Val. Energy management in solar thermal power plants with double thermal storage system and subdivided solar field. *Applied Energy*, 88:4055–4066, 2011.

[13] J. Sanz-Bermejo, V. Gallardo-Natividad, J. Gonzalez-Aguilar, and M. Romero. Comparative system performance analysis of direct steam

generation central receiver solar thermal power plants in megawatt range. *Journal of Solar Energy Engineering*, 136:(9 Pages), 2014.

[14] J. G. Broze, S. Ranade, and H. W. Prengle. An approximate model for sizing and costing a solar thermal collector-central receiver system. *Solar Energy*, 34:341–350, 1985.

[15] F. J. Collado and J. Guallar. Campo: Generation of regular heliostat fields. *Renewable Energy*, 46:49–59, 2012.

[16] R. Buck, C. Barth, M. Eck, and W. Steinmann. Dual receiver concept for solar tower. *Solar Energy*, 80:1249–1254, 2006.

[17] A. Segal and M. Epstein. Comparative performances of tower-top and tower-reflector central solar receivers. *Solar Energy*, 65:207–226, 1999.

[18] R. Ben-Zvi, M. Epstein, and A. Segal. Simulation of an integrated steam generator for solar tower. *Solar Energy*, 86:578–592, 2012.

[19] L. Crespo and F. Ramos. NSPOC: A New Powerful Tool for Heliostat Field Layout and Receiver Geometry Optimizations. In *Proceedings of SolarPaces 2009*, September 2009.

[20] A. Sánchez-González and D. Santana. Solar flux distribution on central receivers: A projection method from analytic function. *Renewable Energy*, 74:576–587, 2014.

[21] J. Bang-Jensen, G. Gutin, and A. Yeo. When the greedy algorithm fails. *Discrete Optimization*, 1:121–127, 2004.

[22] G. Ausiello, P. Crescenzi, G. Gambosi, V. Kann, A. Marchetti-Spaccamela, and M. Protasi. *Complexity and Approximation*. Springer, Berlin, 1999.

[23] V. V. Vazirani. *Approximation algorithms*. Springer Science & Business Media, 2013.

[24] J-F. Cordeau, M. Gendreau, G. Laporte, J-Y. Potvin, and F. Semet. A guide to vehicle routing heuristics. *The Journal of the Operational Research Socitey*, 53:512–522, 2002.

[25] S. Guha and S. Khuller. Greedy strikes back: Improved facility location algorithms. *Journal of Algorithms*, 31(1):228–248, 1999.

[26] E. Carrizosa, C. Domínguez-Bravo, E. Fernández-Cara, and M. Quero. An optimization approach to the design of multi-size heliostat fields. Technical report, IMUS, 2014. URL `www.optimization-online.org/DB_HTML/2014/05/4372.html`.

[27] E. Leonardi and B. D'Aguanno. Crs4-2: A numerical code for the calculation of the solar power collected in a central receiver system. *Energy*, 36:4828–4837, 2011.

[28] E. Carrizosa, C. Domínguez-Bravo, E. Fernández-Cara, and M. Quero. A heuristic method for simultaneous tower and pattern-free field optimization on solar power systems. *Computers & Operations Research*, 57:109–122, 2015.

[29] F. J. Collado and J.A. Turégano. Calculation of the annual thermal

energy supplied by a defined heliostat field. *Solar Energy*, 42:149–165, 1989.

[30] M. Izygon, P. Armstrong, N. Nilsson, and N. Vu. TieSOL – a GPU-based suite of fsoftware for central receiver solar power plants. In *Inproceedings of SolarPaces 2011*, 2011.

[31] M. S. Bazaraa, H. D. Sherali, and C. M. Shetty. *Nonlinear Programming: Theory and Algorithms*. John Wiley and Sons, Hoboken, New Jersey, 2006.

[32] C. J. Noone, M. Torrilhon, and A. Mitsos. Heliostat field optimization: A new computationally efficient model and biomimetic layout. *Solar Energy*, 86:792–803, 2012.

[33] R. Buck. Heliostat field layout improvement by nonrestricted refinement. *Journal of Solar Energy Engineering*, 136(021014):(6 Pages), 2014.

[34] B. Belhomme, R. Pitz-Paal, and P. Schwarzbözl. Optimization of heliostat aim point selection for central receiver systems based on the ant colony optimization metaheuristic. *Journal of Solar Energy Engineering*, 136(011005):(7 Pages), 2014.

[35] A. Kribus, I. Vishnevetsky, A. Yogev, and T. Rubinov. Closed loop control of heliostats. *Energy*, 29:905–913, 2004.

[36] J. Spelling, D. Favrat, A. Martin, and G. Augsburger. Thermoeconomic optimization of a combined-cycle solar tower power plant. *Energy*, 41: 113–120, 2012.

[37] P. Schramek, D. R. Mills, W. Stein, and P. Le Livre. Design of the Heliostat Field of the CSIRO Solar Tower. *Journal of Solar Energy Engineering*, 131(024505):(6 Pages), 2009.

[38] R. Osuna, V. Fernández, S. Romero, M. Romero, and M. Sánchez. PS10: a 11.0-MWe Solar Tower Power Plant with Satured Steam Receiver. In *Proceedings of SolarPaces 2004*, 2004. Editors: C. Ramos and J. Huacuz.

Algorithm 1 `Alternating algorithm`

Require: Θ_0 (feasible) and ϵ_0

$k \leftarrow 0$

$\mathcal{S}^0 \leftarrow$ solve $(\mathcal{P}_\Theta)$ given $\Theta = \Theta^0$

$\Upsilon_{obj} \leftarrow F(\Theta^0, \mathcal{S}^0)$

repeat

$k \leftarrow k + 1$

$\Theta^k \leftarrow$ solve $(\mathcal{P}_\mathcal{S})$ given $\mathcal{S} = \mathcal{S}^{k-1}$

$\mathcal{S}^k \leftarrow$ solve $(\mathcal{P}_\Theta)$ given $\Theta = \Theta^k$

$\Upsilon_{obj} = \min\{\Upsilon_{obj}, F(\Theta^k, \mathcal{S}^{k-1}), F(\Theta^k, \mathcal{S}^k)\}$

until $||F(\Theta^k, \mathcal{S}^k) - F(\Theta^{k+1}, \mathcal{S}^{k+1})|| \leq \epsilon_0$

return Υ_{obj} (best objective value and configuration)

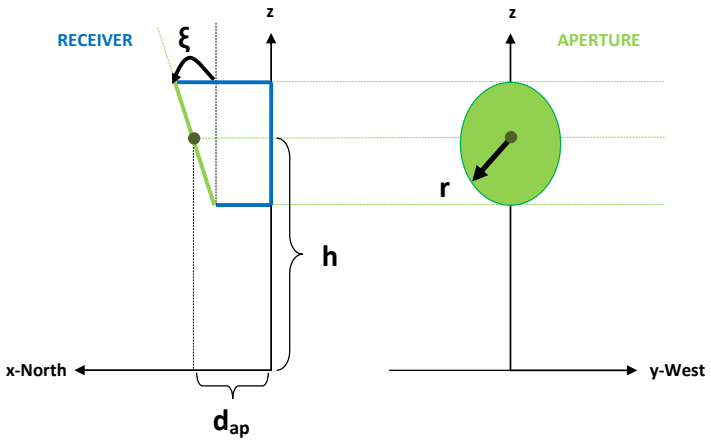

(a) h, ξ angle and r (front-lateral)

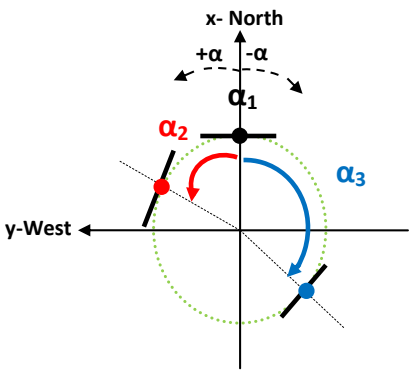

(b) α angle (top)

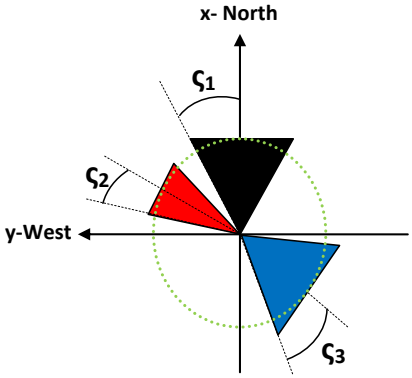

(c) ς angle (top)

Figure 1: Receivers variables

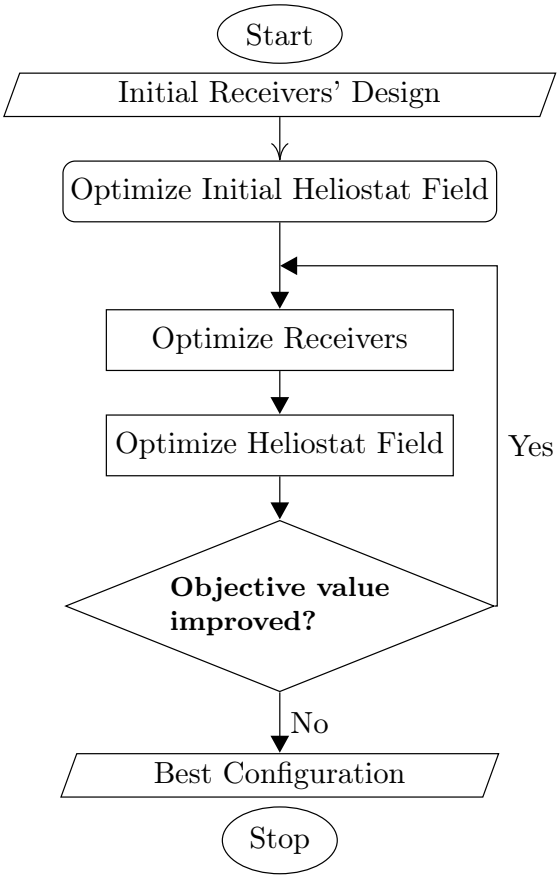

Figure 2: Diagram for the alternating algorithm

Algorithm 2 `Multiple Receivers Algorithm`

Require: Π_i^-, $\mathcal{S}$, ϵ_1 and Θ^0 (feasible)

$k \leftarrow 0$

$F_0 \leftarrow F(\Theta^0, \mathcal{S})$

$\Upsilon_{obj} \leftarrow F_0$

repeat

$k \leftarrow k + 1$

for $i = 1 : 3$ **do**

$h_i^k \leftarrow$ solve $\max_{h_i} F(\Theta, \mathcal{S})$ with $h_i \in [r_i, h_{max}]$

$\xi_i^k \leftarrow$ solve $\max_{\xi_i} F(\Theta, \mathcal{S})$ with $\xi_i \in [0, \pi/2]$

$\alpha_i^k \leftarrow$ solve $\max_{\alpha_i} F(\Theta, \mathcal{S})$ with $\alpha_i \in [\underline{\alpha}_i, \overline{\alpha}_i]$

$r_i^k \leftarrow$ solve $\max_{r_i} F(\Theta, \mathcal{S})$ with $r_i \in [r_{min}, \min(h_i, r_{max})]$

$\Theta_i^k \leftarrow (h_i^k, \xi_i^k, \alpha_i^k, r_i^k)$

end for

$\Theta^k \leftarrow (\Theta_1^k, \Theta_2^k, \Theta_3^k)$

$F_k \leftarrow F(\Theta^k, \mathcal{S})$

$\Upsilon_{obj} = \min\{\Upsilon_{obj}, F(\Theta^k, \mathcal{S})\}$

until $F_k > F_{k-1}$ or $||\Theta^k - \Theta^{k+1}||_\infty \leq \epsilon_1$

return Υ_{obj} (best objective value and configuration)

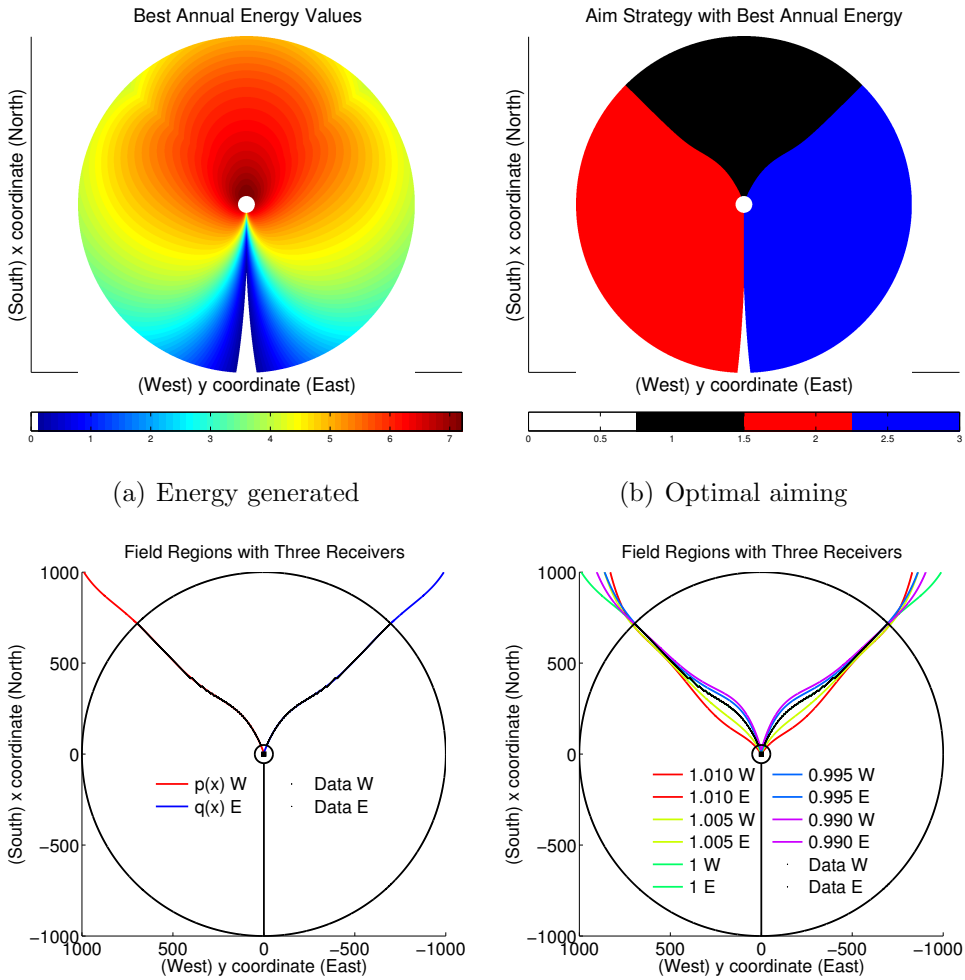

(a) Energy generated

(b) Optimal aiming

(c) Aiming regions for $w = 1$

(d) Aiming regions for several w

Figure 3: Aiming regions calculation

Algorithm 3 `Heliostat location Algorithm for multiple receivers`

Require: Θ, Ω

$\mathcal{S} = \emptyset$ Requirement Phase

$k \leftarrow 0$

for $i = 1, 2, 3$ **do**

  while $\Pi_{T_d}(\Theta, \mathcal{S}_i) < \Pi_i^-$ **do**

    $k \leftarrow k + 1$

    $(x^k, y^k) \leftarrow$ solve $\left(\mathcal{P}_\Theta^i\right)^k$ with Greedy Alg.

    $\mathcal{S}_i \leftarrow \mathcal{S}_i \cup \{(x^k, y^k)\}$

  end while

  $\mathcal{S} \leftarrow \mathcal{S} \cup \mathcal{S}_i$

end for

$\mathcal{S}^k \leftarrow \mathcal{S}$ Completion Phase

repeat

  $k \leftarrow k + 1$

  for $i = 1, 2, 3$ **do**

    $(x_i^k, y_i^k) \leftarrow$ solve $\left(\mathcal{P}_\Theta^i\right)^k$ with Greedy Alg.

    $\mathcal{S}_i^k \leftarrow \mathcal{S}^k \cup \{(x_i^k, y_i^k)\}$

  end for

  $j \leftarrow \max_i\{E(\Theta, \mathcal{S}_i^k)\}$

  $\mathcal{S}^k \leftarrow \mathcal{S}_j^k$

until $F(\Theta, \mathcal{S}^k) > F(\Theta, \mathcal{S}^{k-1})$ or $\Pi_{T_d}(\Theta_i, \mathcal{S}^k) > \Pi_i^+$ for $i \in [1, 2, 3]$

return $\mathcal{S}^{k-1}$ (final field)

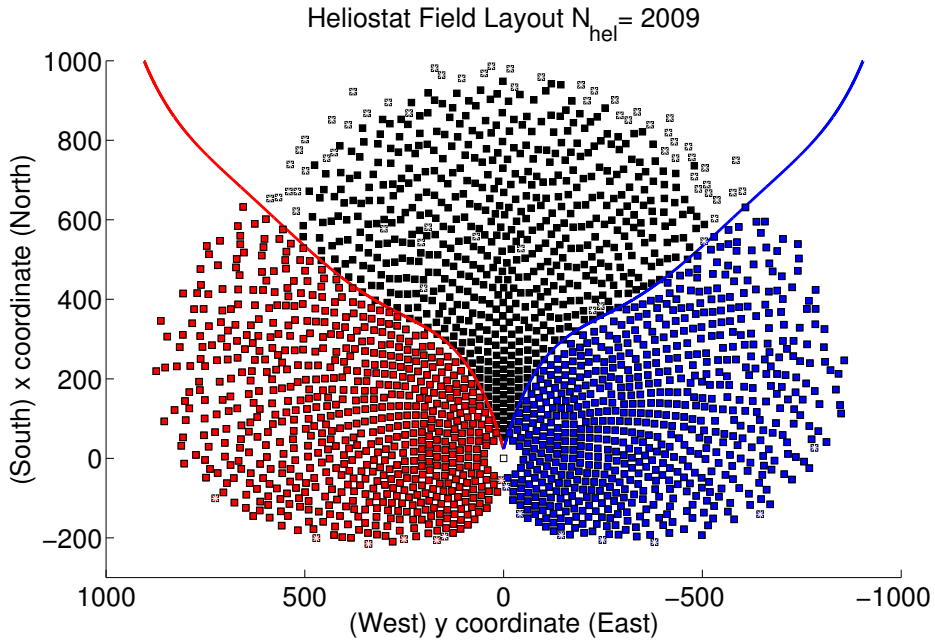

(a) $\mathcal{S}^0$ with $w = 0.990$ and Θ^0 fixed

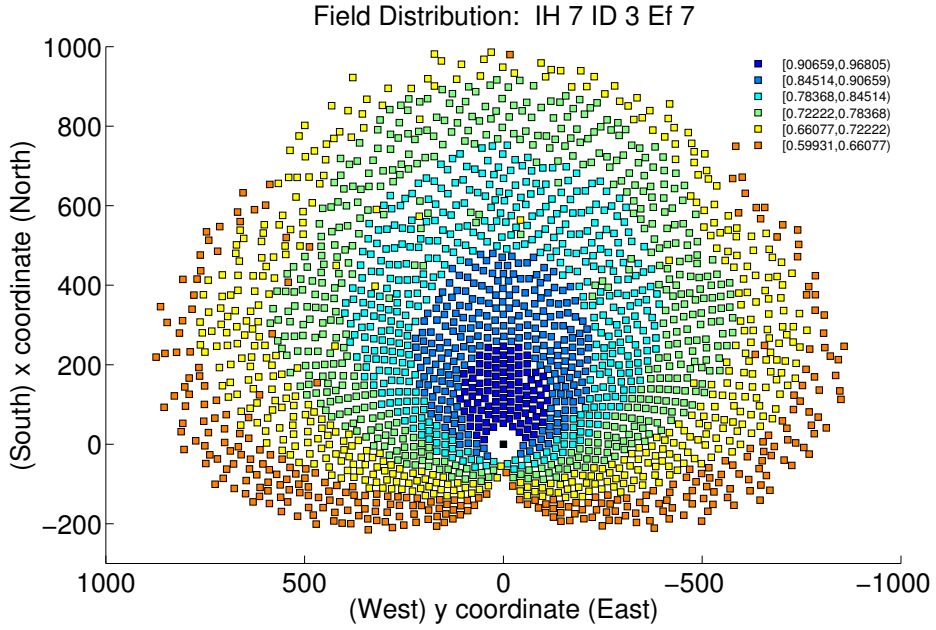

(b) $\mathcal{S}^0$ (21st March 12 h)

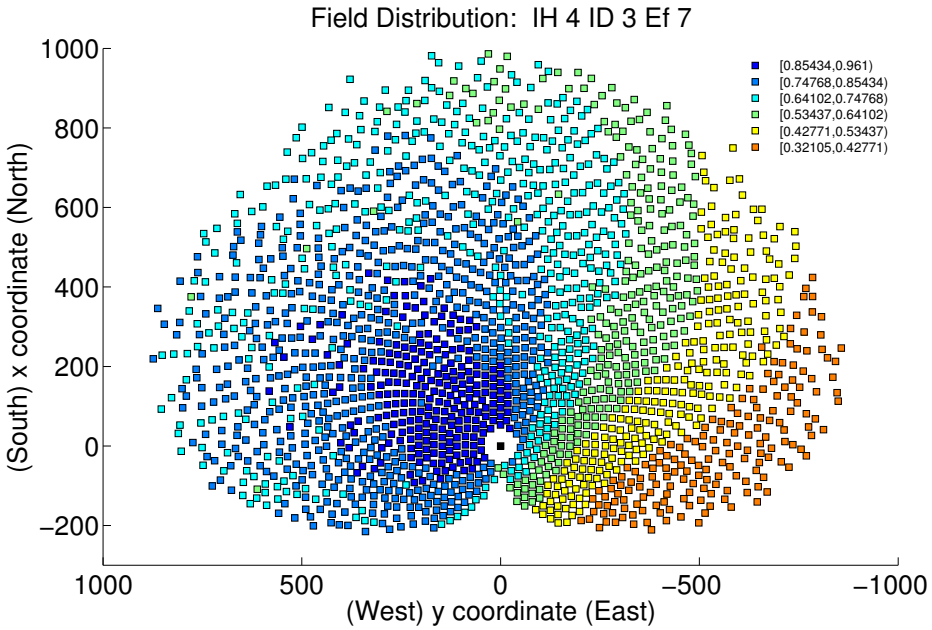

(c) $\mathcal{S}^0$ (21st March 09 h)

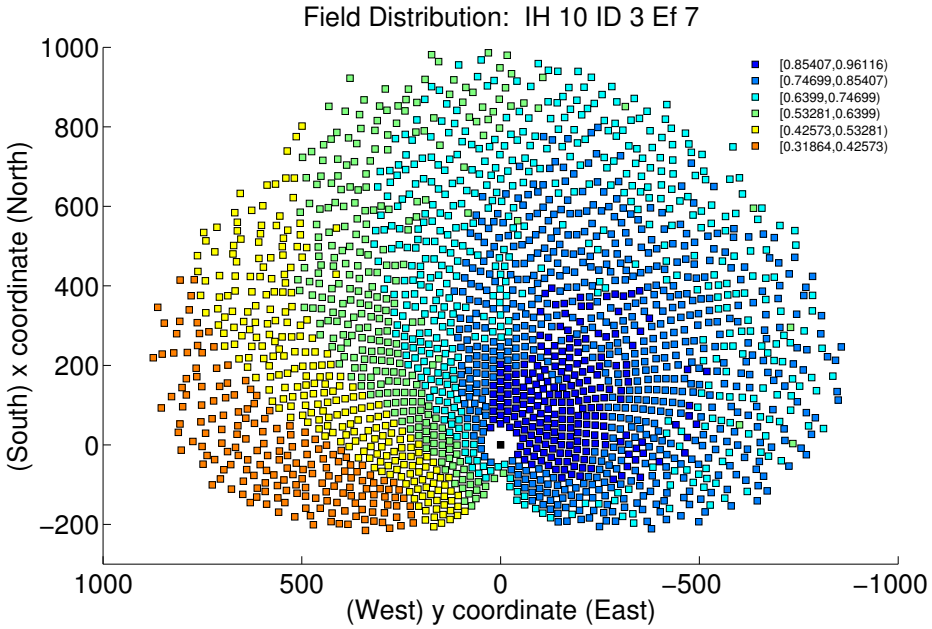

(d) $\mathcal{S}^0$ (21st March 15 h)

Figure 4: Heliostat Field $\mathcal{S}^0$ and Efficiency Coefficient

Table 1: Parameter Values

Parameter	Default value	Ref.
Location and Time		
Site	Sanlúcar la Mayor (Seville)	[38]
Latitude	$37^o26'$ N	[32]
Longitude	$6^o15'$ W	[32]
Design Point T_d	March Day 21 Hour 12	assumed
Design direct normal irradiance DNI	823.9 W/m^2	assumed
DNI model	cloudless sky	assumed
Heliostat		
Name	$Sanlucar120$	[32]
Width	12.84 m	[32]
Height	9.45 m	[32]
Optical height z_0	5.17 m	[38]
Minimal safety distance δ	heliostat diagonal+d_s	[33]
$\sigma_{optical}$	2.9 mrad	[32]
Field		
Slope	0^o	assumed
Shape	annulus	assumed
Minimum radius	50 m	assumed
Maximum radius	10^3 m	assumed

Table 2: Alternating Algorithm Results: Receiver

Step		h [m]	ξ [grad]	α [grad]	r [m]
Θ^0	Θ_1	100.50	12.50	0	6.39
	Θ_2	100.50	12.50	90	6.39
	Θ_3	100.50	12.50	-90	6.39
Θ^1	Θ_1	100.53	8.72	-0.81	4.83
	Θ_2	100.50	17.24	80.94	4.44
	Θ_3	100.50	17.96	-81.32	4.48
Θ^2	Θ_1	100.50	10.71	-0.26	4.44
	Θ_2	100.50	17.50	75.41	4.11
	Θ_3	100.50	17.43	-76.09	4.11

Table 3: Alternating Algorithm Results: Configurations

Step	Pb	$\lvert\mathcal{S}\rvert$	Π_{T_d} [MWth]	E [GWHth]	C [M€]	C/E
$k=0$	$1:(\Theta^0,\mathcal{S}^0)$	2009	118.7550	326.83	5.9984	0.01835
	$2:(\Theta^1,\mathcal{S}^0)$	2009	112.0731	310.62	5.3916	0.01736
$k=1$	$3:(\Theta^1,\mathcal{S}^1)$	2033	115.0178	314.55	5.4445	0.01731
	$4:(\Theta^2,\mathcal{S}^1)$	2033	110.4583	306.45	5.3443	0.01744
$k=2$	$5:(\Theta^2,\mathcal{S}^2)$	2084	114.8432	312.30	5.4567	0.01747

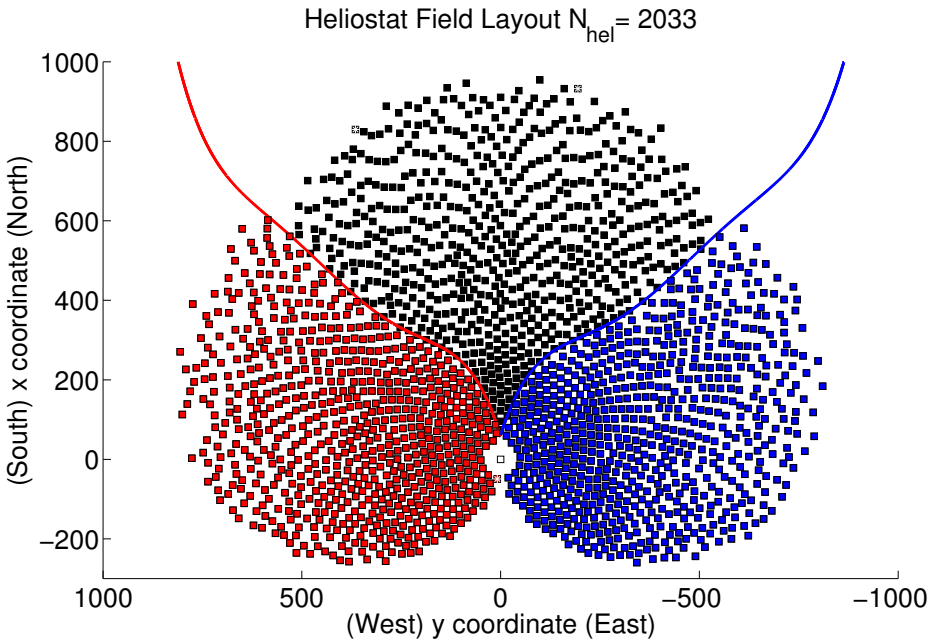

(a) $\mathcal{S}^1$ (Θ^1 fixed) Final Field

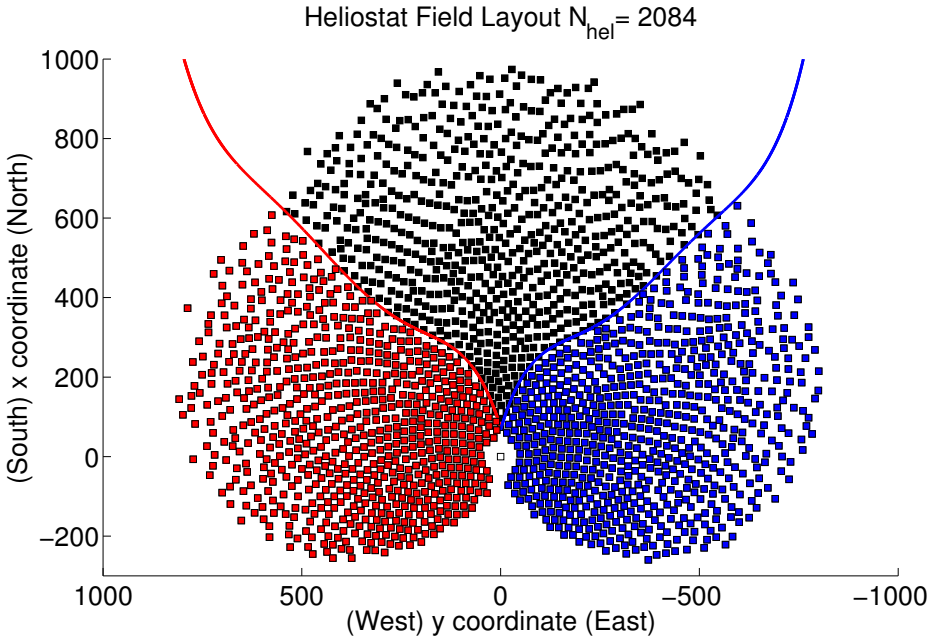

(b) $\mathcal{S}^2$ (Θ^2 fixed)

Figure 5: Heliostat Fields

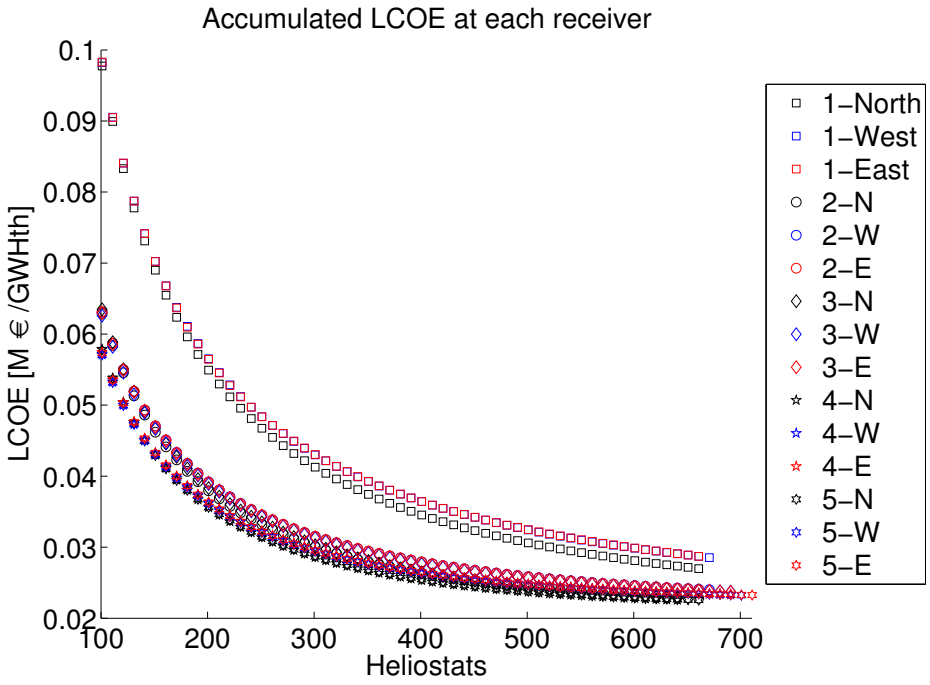

Figure 6: Alternating Process: LCOE (M€/GWHth)